21st International Symposium on
Mathematical Theory of Networks and Systems
July 7-11, 2014. Groningen, The Netherlands

A Port-Hamiltonian Finite-Element Formulation for the Transmission Line*

Ortwin Farle[1], Rolf-Björn Baltes[1], and Romanus Dyczij-Edlinger[1]

***Abstract*— This paper presents a new port-Hamiltonian formulation for the transmission line. By eliminating the dual complex from the underlying Dirac structure, it enables structure-preserving spatial semi-discretization using mixed finite elements. The proposed discretization scheme preserves not only the port-Hamiltonian structure but also important conservation laws. A numerical example using the p version of the finite element method demonstrates the improvements in convergence attainable by higher-order discretization schemes.**

***Index Terms*— Port-Hamiltonian systems; spatial semi-discretization; finite element methods.**
***AMS subject classifications*– 37K05, 65N30**

I. INTRODUCTION

Port-Hamiltonian formulations provide a unifying framework for the energy-based modeling of both lumped- [1], [2] and distributed-parameter systems [3], [4]. This contribution addresses the structure-preserving finite-dimensional approximation of distributed-parameter systems. The transmission line serves as a canonical model problem.

Existing methods [5], [6], [7] use the Stokes Dirac structure presented in [3] and model the transmission line as a system of two coupled conservation laws. In the framework of *'generalized finite differences'* [8], this naturally leads to discretizating the two complexes by a primal and a dual mesh [7], respectively. However, this approach is unsuitable for the finite element (FE) method, which employs weak forms in place of the dual mesh.

Adopting an idea from [9], we introduce a new metric-dependent Dirac structure and derive a modified port-Hamiltonian formulation for the distributed-parameter system. It bypasses the dual complex and, thus, enables discretization by mixed FE's [10]. We will show that FE discretization preserves not only the Port-Hamiltonian structure but also various conservation properties of the original distributed-parameter system. The numerical example of Section IV demonstrates that the p version of the FE method achieves significant improvements in convergence rate, compared to existing approaches [5], [6], [7].

II. DIRAC STRUCTURE

For completeness, we restate the definition of a Dirac structure given in [3]: Let $f \in \mathcal{F}$ and $e \in \mathcal{E}$, where $\mathcal{F}$ and $\mathcal{E}$ denote linear spaces. We consider a bilinear pairing

$$\langle e|f\rangle : \mathcal{F} \times \mathcal{E} \to \mathbb{R} \tag{1}$$

and its symmetrization $\langle\langle\cdot|\cdot\rangle\rangle : (\mathcal{F}\times\mathcal{E})\times(\mathcal{F}\times\mathcal{E}) \to \mathbb{R}$,

$$\langle\langle (f^1,e^1)|(f^2,e^2)\rangle\rangle := \langle e^1|f^2\rangle + \langle e^2|f^1\rangle. \tag{2}$$

Definition 1: Let $\mathcal{F}$ and $\mathcal{E}$ be linear spaces with the pairing (1). A *Dirac structure* is a linear subspace $\mathcal{D} \subset \mathcal{F}\times\mathcal{E}$ such that $\mathcal{D} = \mathcal{D}^\perp$, with $\perp$ denoting the orthogonal complement with respect to the bilinear form (2).

As usual, we denote by $\mathcal{F}$ the space of flows f and by $\mathcal{E}$ the space of efforts e [11]. Thus, if (f,e) is a pair of power variables [11], then $(f,e) \in \mathcal{D}$ represents power conservation [3].

Let $\Omega \subset \mathbb{R}$ be an open interval of the real axis with boundary $\partial\Omega$, $\Lambda^k(\Omega)$ with $k \in \{0,1\}$ the space of exterior k-forms on Ω [12], and $\Lambda^0(\partial\Omega)$ the space of exterior 0-forms on $\partial\Omega$. The wedge product of differential forms $\wedge : \Lambda^k \times \Lambda^p \to \Lambda^{k+p}$ represents the natural pairing $\langle\cdot|\cdot\rangle_M : \Lambda^k(M)\times\Lambda^{m-k}(M)\to\mathbb{R}$,

$$\langle\omega|\eta\rangle_M := \int_M \omega\wedge\eta, \tag{3}$$

where M is an m dimensional manifold. Note that the pairing is non-degenerate, i.e. if $\langle\omega|\eta\rangle = 0$ for all η, then $\omega = 0$ on M.

To model the transmission line, we introduce the spaces

$$\mathcal{F} := \Lambda^0(\Omega)\times\Lambda^1(\Omega)\times\Lambda^0(\partial\Omega)\times\Lambda^d(S), \tag{4a}$$
$$\mathcal{E} := \Lambda^1(\Omega)\times\Lambda^0(\Omega)\times\Lambda^0(\partial\Omega)\times\Lambda^{s-d}(S), \tag{4b}$$

where S is an s-dimensional manifold and $d \in \{0,\dots,s\}$. The manifold S corresponds to distributed ports which will be used to incorporate energy dissipation. Symmetrizing the pairing (3) gives the bilinear form $\langle\langle\cdot|\cdot\rangle\rangle : (\mathcal{F}\times\mathcal{E})\times(\mathcal{F}\times\mathcal{E})\to\mathbb{R}$,

$$\begin{aligned}\langle\langle (f^1,e^1)|(f^2,e^2)\rangle\rangle :=& \\ &\int_\Omega \left(e_1^1\wedge f_1^2 + e_2^1\wedge f_2^2 + e_1^2\wedge f_1^1 + e_2^2\wedge f_2^1\right) \\ +\int_{\partial\Omega}(e_b^1\wedge f_b^2 + e_b^2\wedge f_b^1) &+ \int_S (e_d^1\wedge f_d^2 + e_d^2\wedge f_d^1),\end{aligned} \tag{5}$$

where, for $i\in\{1,2\}$, we have

$$f^i = (f_1^i, f_2^i, f_b^i), \qquad e^i = (e_1^i, e_2^i, e_b^i), \tag{6a}$$
$$f_1^i \in \Lambda^0(\Omega), \qquad e_1^i \in \Lambda^1(\Omega), \tag{6b}$$
$$f_2^i \in \Lambda^1(\Omega), \qquad e_2^i \in \Lambda^0(\Omega), \tag{6c}$$
$$f_b^i \in \Lambda^0(\partial\Omega), \qquad e_b^i \in \Lambda^0(\partial\Omega), \tag{6d}$$
$$f_d^i \in \Lambda^d(S), \qquad e_d^i \in \Lambda^{s-d}(S). \tag{6e}$$

*This work was supported in part by grant DY 112/1-1 of the Deutsche Forschungsgemeinschaft (DFG).

[1]The authors are with Chair for Electromagnetic Theory, Faculty of Physics and Mechatronics, Saarland University, Saarbrücken, D-66123, Germany. o.farle@lte.uni-saarland.de

Before stating the new Dirac structure, let us introduce some notation: We denote the restriction of $\omega \in \Lambda^1(\Omega)$ to the boundary $\partial\Omega$ by $\omega|_{\partial\Omega}$, the exterior derivative by d, and the Hodge operator by $*$ [12]. To model energy exchange through the distributed ports, we define the linear map

$$G = \begin{bmatrix} G_1 \\ G_2 \end{bmatrix} : \Lambda^d(S) \to \Lambda^0(\Omega) \times \Lambda^1(\Omega) \tag{7}$$

and its dual map

$$G^* = (G_1^*, G_2^*) : \Lambda^1(\Omega) \times \Lambda^0(\Omega) \to \Lambda^{s-d}(S), \tag{8}$$

satisfying

$$\begin{aligned} &\int_\Omega \left[e_1 \wedge G_1(f_d) + e_2 \wedge G_2(f_d)\right] \\ &\qquad = \int_S \left[G_1^*(e_1) + G_2^*(e_2)\right] \wedge f_d \qquad \forall e_1, e_2, f_d. \end{aligned} \tag{9}$$

Theorem 2: Given the spaces $\mathcal{F}$ and $\mathcal{E}$ of (4) and the bilinear form $\langle\!\langle \cdot | \cdot \rangle\!\rangle$ of (5), define a linear subspace $\mathcal{D}$ of $\mathcal{F} \times \mathcal{E}$ by:

$$\begin{aligned} \mathcal{D} := \Big\{ (f_1, f_2, f_b, f_d, e_1, e_2, e_b, e_d) \in \mathcal{F} \times \mathcal{E} \,\Big|\, & \\ \begin{bmatrix} f_1 \\ f_2 \end{bmatrix} &= \begin{bmatrix} 0 & *\mathrm{d} \\ \mathrm{d}* & 0 \end{bmatrix} \begin{bmatrix} e_1 \\ e_2 \end{bmatrix} + G(f_d), \\ \begin{bmatrix} e_b \\ f_b \end{bmatrix} &= \begin{bmatrix} -* & 0 \\ 0 & 1 \end{bmatrix} \begin{bmatrix} e_1|_{\partial\Omega} \\ e_2|_{\partial\Omega} \end{bmatrix}, \\ e_d &= -G^* \begin{bmatrix} e_1 \\ e_2 \end{bmatrix} \Big\}. \end{aligned} \tag{10}$$

Then $\mathcal{D}$ is a Dirac structure.

Proof: See Appendix I. ∎

III. APPLICATION TO TRANSMISSION LINE SYSTEMS

A. Infinite-Dimensional System

Without loss of generality, we consider a transmission line of length l with $\Omega = (0, l)$. Under the assumption of linear time-invariant material properties the Hamiltonian density $\mathcal{H}$ can be written as

$$\mathcal{H} = \frac{1}{2} *_L i \wedge i + \frac{1}{2} *_{C^{-1}} q \wedge q, \tag{11}$$

where $i \in \Lambda^0(\Omega)$ denotes the electric current, $q \in \Lambda^1(\Omega)$ the electric charge density, and $*_L$, $*_{C^{-1}}$ the positive definite Hodge operators representing the distributed inductance and the inverse distributed capacitance, respectively. The total energy $H \in \mathbb{R}$ is given by $H = \int_\Omega \mathcal{H}$. Following the framework described in Section 2.3 of [3], we obtain the effort and flow variables

$$e_1 = \delta_i H = *_L i = \phi, \tag{12a}$$

$$e_2 = \delta_q H = *_{C^{-1}} q = v, \tag{12b}$$

$$f_1 = -\frac{\partial i}{\partial t} = -\frac{\partial (*_{L^{-1}} \phi)}{\partial t}, \tag{12c}$$

$$f_2 = -\frac{\partial q}{\partial t} = -\frac{\partial (*_C v)}{\partial t}, \tag{12d}$$

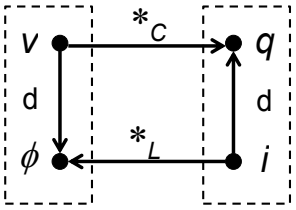

Fig. 1. Relations between function spaces.

where $\phi \in \Lambda^1(\Omega)$ and $v \in \Lambda^0(\Omega)$ stand for the magnetic flux density and the electric voltage, respectively. The variational derivative [13] of H with respect to x is denoted by $\delta_x H$. Fig. 1 illustrates the relations between the function spaces. The two disjoint complexes are arranged horizontally. They are connected via the metric-dependent Hodge operators which represent the constitutive laws.

The first equation of (10) reads

$$-\frac{\partial}{\partial t} \begin{bmatrix} *_{L^{-1}} \phi \\ *_C v \end{bmatrix} = \begin{bmatrix} 0 & *_{L^{-1}} \mathrm{d} \\ \mathrm{d} *_{L^{-1}} & 0 \end{bmatrix} \begin{bmatrix} \phi \\ v \end{bmatrix}, \tag{13}$$

with the state vector

$$x = -\begin{bmatrix} *_{L^{-1}} \phi \\ *_C v \end{bmatrix}. \tag{14}$$

The first row of (13) states conservation of magnetic flux Φ:

$$\frac{\mathrm{d}}{\mathrm{d}t}\Phi = \frac{\mathrm{d}}{\mathrm{d}t} \int_\Omega \phi \overset{(13)}{=} -\int_\Omega \mathrm{d}v = v(0) - v(l), \tag{15}$$

and the second row implies conservation of electric charge Q:

$$\frac{\mathrm{d}}{\mathrm{d}t} Q = \frac{\mathrm{d}}{\mathrm{d}t} \int_\Omega q \overset{(13)}{=} -\int_\Omega \mathrm{d} *_{L^{-1}} \phi = i(0) - i(l). \tag{16}$$

The system is excited by imposing a current $i = -e_b$ at $\partial\Omega$. The corresponding output is the voltage $v = f_b$. For the change in energy, we obtain

$$\frac{\mathrm{d}H}{\mathrm{d}t} = \int_{\partial\Omega} e_b \wedge f_b = i(0)v(0) - i(l)v(l). \tag{17}$$

B. Finite-Dimensional Approximation

We only discretize the complex on the left side of Fig. 1, which will be denoted the primal complex. On the one-dimensional manifold Ω, 0-forms and 1-forms are approximated by means of H^1 and H^0-conforming FE shape functions [12], respectively. The first row of (13) is discretized in strong form, because v and ϕ reside on the primal complex, and $*_{L^{-1}}$ is applied to both sides of the equation. The exterior derivative is represented by the discrete derivative operator $\mathbf{D} \in \mathbb{R}^{N_e \times N_n}$ [8], where N_e and N_n are the dimensions of the H^0 and H^1-conforming FE spaces, respectively. The discrete counterpart of the Hodge operator $*_{L^{-1}}$ is the mass matrix $\mathbf{T}_{L^{-1}} \in \mathbb{R}^{N_n \times N_n}$ of H^0-conforming shape functions [14]. The quantities on the second row of (13) live on the dual complex and must therefore be discretized in weak form, by formally applying the integration-by-parts formula

$$\int_\Omega \alpha \wedge \mathrm{d} *_{L^{-1}} \phi = \int_{\partial\Omega} \alpha \wedge *_{L^{-1}} \phi - \int_\Omega \mathrm{d}\alpha \wedge *_{L^{-1}} \phi, \tag{18}$$

where $\alpha \in \Lambda^0(\Omega)$. The boundary term in (18) is an imposed quantity and corresponds to the excitation. Its discrete version $\mathbf{Bi} \in \mathbb{R}^{N_n}$, with $\mathbf{i} = [i(0)\ i(l)]^T$, describes the input of the system

$$\mathbf{E}\frac{\mathrm{d}}{\mathrm{d}t}\mathbf{x} = \mathbf{J}\mathbf{x} + \mathbf{G}\mathbf{i}, \tag{19a}$$

$$\mathbf{v} = \mathbf{G}^T\mathbf{x}, \tag{19b}$$

where

$$\mathbf{x} = \begin{bmatrix}\mathbf{x}_\phi \\ \mathbf{x}_v\end{bmatrix}, \qquad \mathbf{J} = \begin{bmatrix}\mathbf{0} & -\mathbf{T}_{L^{-1}}\mathbf{D} \\ \mathbf{D}^T\mathbf{T}_{L^{-1}} & \mathbf{0}\end{bmatrix}, \tag{20a}$$

$$\mathbf{G} = \begin{bmatrix}\mathbf{0} \\ \mathbf{B}\end{bmatrix}, \qquad \mathbf{E} = \begin{bmatrix}\mathbf{T}_{L^{-1}} & \mathbf{0} \\ \mathbf{0} & \mathbf{T}_C\end{bmatrix}, \tag{20b}$$

$$\mathbf{v} = \begin{bmatrix}v(0) \\ v(l)\end{bmatrix}. \tag{20c}$$

Here $\mathbf{T}_C \in \mathbb{R}^{N_n \times N_n}$ is the mass matrix of H^1-conforming shape functions, representing $*_C$. The vectors $\mathbf{x}_\phi \in \mathbb{R}^{N_e}$ and $\mathbf{x}_v \in \mathbb{R}^{N_n}$ correspond to the degrees of freedom (DoF) for ϕ and v.

Proposition 3: The discrete system (19) preserves the conservation law (15).

Proof: We need to introduce some notation: The discrete magnetic flux density ϕ is given by

$$\phi(x) = \sum_{i=1}^{N_e} x_\phi^i w_i(x), \tag{21}$$

where $w_i(x)$ is an H^0-conforming shape function, and x_ϕ^i is the i-th entry of the vector $\mathbf{x}_\phi$. The entries of the discrete derivative operator $\mathbf{D}$ are denoted by d_{ij}. With the help of $\mathbf{D}$, the derivative of the H^1-conforming shape functions $N_k(x)$ is expressed by a superposition of H^0-conforming shape functions $w_i(x)$:

$$\frac{\mathrm{d}}{\mathrm{d}x}N_k(x) = \sum_{i=1}^{N_e} d_{ik} w_i(x). \tag{22}$$

We are now ready to compute the time derivative of the discrete approximation of the magnetic flux:

$$\begin{aligned}
\frac{\mathrm{d}}{\mathrm{d}t}\Phi &\overset{(21)}{=} \frac{\mathrm{d}}{\mathrm{d}t}\int_0^l \sum_{i=1}^{N_e} x_\phi^i w_i(x)\,\mathrm{d}x \\
&\overset{(19)}{=} -\int_0^l \sum_{i=1}^{N_e}\sum_{k=1}^{N_n} x_v^k d_{ik} w_i(x)\,\mathrm{d}x \\
&\overset{(22)}{=} \int_0^l \sum_{k=1}^{N_n} x_v^k \frac{\mathrm{d}}{\mathrm{d}x}N_k(x)\,\mathrm{d}x \\
&= -\sum_{k=1}^{N_n} x_v^k \left[N_k(x)\right]_0^l \\
&= v(0) - v(l).
\end{aligned} \tag{23}$$

■

The second row of (19a) corresponds to the weak form of the second row of (13). Thus the conservation law (16) is only preserved in the weak sense.

Since we have not discretized the state variables, (19) does not look like a standard port-Hamiltonian system [1]. It is brought to standard form by substituting

$$\mathbf{x}_i = \mathbf{T}_{L^{-1}}\mathbf{x}_\phi, \tag{24a}$$

$$\mathbf{x}_q = \mathbf{T}_C\mathbf{x}_v. \tag{24b}$$

With the modified state vector

$$\hat{\mathbf{x}} = \begin{bmatrix}\mathbf{x}_i \\ \mathbf{x}_q\end{bmatrix}, \tag{24c}$$

the system (19) is rewritten as

$$\frac{\mathrm{d}}{\mathrm{d}t}\hat{\mathbf{x}} = \mathbf{J}\nabla H(\hat{\mathbf{x}}) + \mathbf{g}\mathbf{i}, \tag{25a}$$

$$\mathbf{v} = \mathbf{g}^T\nabla H(\hat{\mathbf{x}}), \tag{25b}$$

where

$$\nabla H(\hat{\mathbf{x}}) = \begin{bmatrix}\mathbf{T}_{L^{-1}}^{-1}\mathbf{x}_i \\ \mathbf{T}_C^{-1}\mathbf{x}_q\end{bmatrix}. \tag{26}$$

Note that the Hamiltonian of (25) is not an abstract quantity but corresponds to the physical energy:

$$\begin{aligned}
H &= \frac{1}{2}\hat{\mathbf{x}}^T\begin{bmatrix}\mathbf{T}_{L^{-1}}^{-1} & \mathbf{0} \\ \mathbf{0} & \mathbf{T}_\varepsilon^{-1}\end{bmatrix}\hat{\mathbf{x}} \\
&= \frac{1}{2}\begin{bmatrix}\mathbf{x}_\phi^T & \mathbf{x}_v^T\end{bmatrix}\begin{bmatrix}\mathbf{T}_{L^{-1}} & \mathbf{0} \\ \mathbf{0} & \mathbf{T}_C\end{bmatrix}\begin{bmatrix}\mathbf{T}_{L^{-1}}^{-1} & \mathbf{0} \\ \mathbf{0} & \mathbf{T}_C^{-1}\end{bmatrix} \\
&\qquad \begin{bmatrix}\mathbf{T}_{L^{-1}} & \mathbf{0} \\ \mathbf{0} & \mathbf{T}_C\end{bmatrix}\begin{bmatrix}\mathbf{x}_\phi \\ \mathbf{x}_v\end{bmatrix} \\
&= \frac{1}{2}\mathbf{x}_\phi^T\mathbf{T}_{L^{-1}}\mathbf{x}_\phi + \frac{1}{2}\mathbf{x}_v^T\mathbf{T}_C\mathbf{x}_v \\
&= \frac{1}{2}\int_0^l L^{-1}\phi^2\,\mathrm{d}x + \frac{1}{2}\int_0^l Cv^2\,\mathrm{d}x.
\end{aligned} \tag{27}$$

By utilizing the skew-symmetry of $\mathbf{J}$, it is straight-forward to show that the discrete system (19) preserves the energy balance (17), too.

IV. Numerical Example

We consider a lossless transmission line of length $l = e - 1$, as described in Section 5 of [5]. Its distributed inductance $L(x)$ and capacitance $C(x)$ are given by

$$L(x) = 1/(1+x), \tag{28}$$

$$C(x) = 1/(1+x). \tag{29}$$

We transform (19) to the frequency domain and excite the structure at $x = 0$ by a unit current of frequency $f = 1$. The transmission line is terminated by its wave impedance $R = 1$. The exact voltage distribution $v(x)$ and magnetic flux density $\phi(x)$ are known to be

$$v(x) = e^{-\mathrm{j}2\pi f \ln(x+1)}, \tag{30}$$

$$\phi(x) = \frac{-1}{x+1}e^{-\mathrm{j}2\pi f \ln(x+1)}. \tag{31}$$

To assess the accuracy of the proposed semi-discretization scheme, we employ the error measure e of [5]:

$$e = |v(1) - v^{FE}(1)|. \tag{32}$$

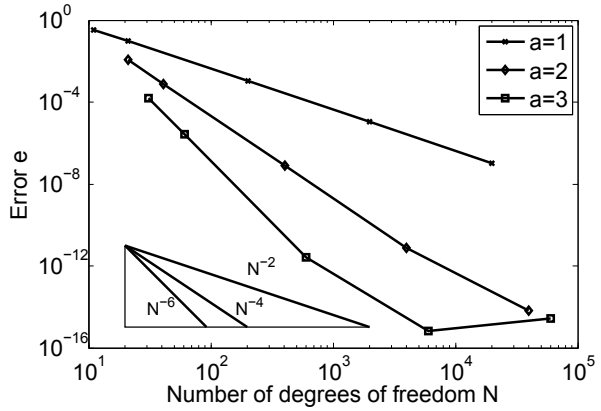

Fig. 2. Voltage error e at $x = 1$ as a function of the number of DoF's, using the order of the FE basis functions a as a parameter.

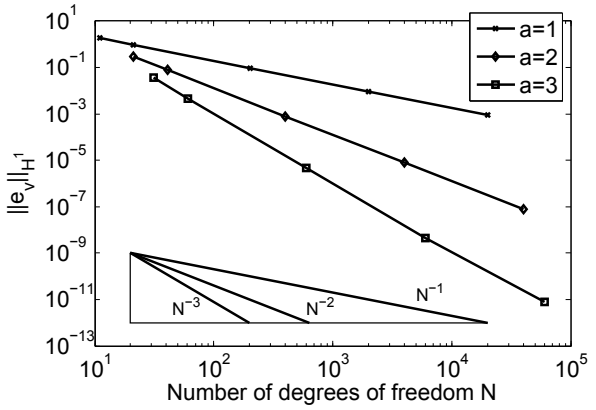

Fig. 3. Error in voltage $\|e_v\|_{H^1}$ as a function of the number of DoF's, using the order of the FE basis functions a as a parameter.

Here v^{FE} denotes the FE approximation to the voltage. Starting from an element size of $h = l/5$, we perform several levels of uniform mesh refinement, by recursively splitting each element into two equal parts. Fig. 2 presents the error (32) as a function of the number of DoF's N, for different orders a of the FE shape functions. In accordance with theoretical predictions [16], the pointwise error in voltage is of order N^{-2a}. Hence, for a given error tolerance, the use of higher-order FEs leads to a significant reduction in the dimension of the discrete model. Saturation at error levels of $10^{-14} \dots 10^{-15}$ is due to numerical noise. We next consider the global error measures

$$\|e_v\|_{H^1} = \left(\int_0^l (|v(x) - v^{FE}(x)|^2 + |\nabla v(x) - \nabla v^{FE}(x)|^2) \, \mathrm{d}x \right)^{1/2}, \quad (33)$$

$$\|e_\phi\|_{H^0} = \left(\int_0^l |\phi(x) - \phi^{FE}(x)|^2 \, \mathrm{d}x \right)^{1/2}, \quad (34)$$

which represent the natural norms of the respective function spaces [15]. Figs. 3 and 4 show the global error measures as functions of the number of DoF's for varying order of the FE shape functions. The respective errors are of order N^{-a}, which again is in agreement with theoretical considerations [16].

V. CONCLUSIONS

A new Dirac structure for the transmission line has been presented. By eliminating the dual complex, it enables the structure-preserving discretization by means of mixed finite elements. It has been shown that energy, magnetic flux and electric charge are conserved in the distributed-parameter system, and how these conservation laws carry over to the discrete system: Energy and magnetic flux are preserved in strong form, whereas electric charge is preserved in weak form. Numerical experiments confirm that the proposed FE scheme attains convergence rates of high order.

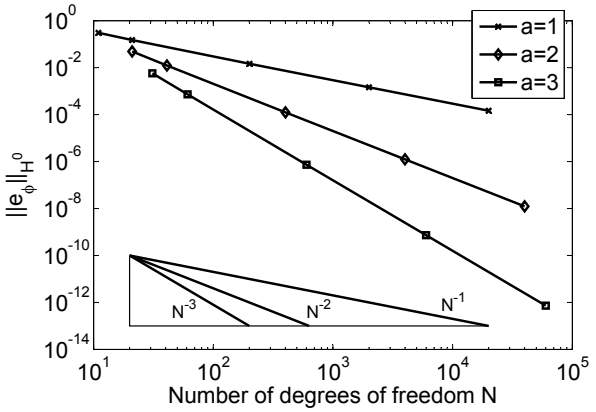

Fig. 4. Error in flux density $\|e_\phi\|_{H^0}$ as a function of the number of DoF's, using the order of the FE basis functions a as a parameter.

APPENDIX I

Proof: The proof is similar to that of Theorem 2.1 in [3] and splits into two parts: (i) $\mathcal{D} \subset \mathcal{D}^\perp$ and (ii) $\mathcal{D}^\perp \subset \mathcal{D}$.

(i) $\mathcal{D} \subset \mathcal{D}^\perp$: Let $(f^1, e^1), (f^2, e^2) \in \mathcal{D}$. By substituting (10) into (5), the right-hand side (r.h.s.) of (5) takes the form

$$\begin{aligned} &\int_\Omega \left[e_1^1 \wedge *\mathrm{d}e_2^2 + e_2^1 \wedge \mathrm{d} * e_1^2 + e_1^2 \wedge *\mathrm{d}e_2^1 + e_2^2 \wedge \mathrm{d}(*e_1^1) \right] \\ &- \int_{\partial\Omega} \left[*e_1^1 \wedge e_2^2 + *e_1^2 \wedge e_2^1 \right] + \int_\Omega \left[e_1^1 \wedge G_1(f_d^2) \right. \\ &\quad \left. + e_2^1 \wedge G_2(f_d^2) + e_1^2 \wedge G_1(f_d^1) + e_2^2 \wedge G_2(f_d^1) \right] \\ &- \int_S \left(G^* \begin{bmatrix} e_1^1 \\ e_1^1 \end{bmatrix} \wedge f_d^2 + G^* \begin{bmatrix} e_1^2 \\ e_2^2 \end{bmatrix} \wedge f_d^1 \right). \end{aligned} \quad (35)$$

The last two integrals cancel because of (9). By utilizing the properties of the exterior derivative and the Hodge operator, we obtain

$$\begin{aligned} \mathrm{d}(*e_1^1 \wedge e_2^2) &= \mathrm{d} * e_1^1 \wedge e_2^2 + *e_1^1 \wedge \mathrm{d}e_2^2 \\ &= e_2^2 \wedge \mathrm{d} * e_1^1 + e_1^1 \wedge *\mathrm{d}e_2^2, \quad (36a) \\ \mathrm{d}(*e_1^2 \wedge e_2^1) &= \mathrm{d} * e_1^2 \wedge e_2^1 + *e_1^2 \wedge \mathrm{d}e_2^1 \\ &= e_2^1 \wedge \mathrm{d} * e_1^2 + e_1^2 \wedge *\mathrm{d}e_2^1. \quad (36b) \end{aligned}$$

Using (36) and Stokes' theorem, we rewrite the first volume integral in (35) as

$$\int_\Omega [\cdots] = \int_{\partial\Omega} \left(*e_1^1 \wedge e_2^2 + *e_1^2 \wedge e_2^1 \right). \tag{37}$$

Therefore, (35) is equal to zero, and $\mathcal{D} \subset \mathcal{D}^\perp$.

(ii) $\mathcal{D}^\perp \subset \mathcal{D}$: Let $(f^1, e^1) \in \mathcal{D}^\perp$. Thus, the r.h.s. of (5) vanishes for all $(f^2, e^2) \in \mathcal{D}$, and (10) implies

$$\begin{aligned}
&\int_\Omega \big[e_1^1 \wedge *\mathrm{d}e_2^2 + e_2^1 \wedge \mathrm{d} * e_1^2 + e_1^2 \wedge f_1^1 + e_2^2 \wedge f_2^1 \\
&\qquad + e_1^1 \wedge G_1(f_d^2) + e_2^1 \wedge G_2(f_d^2) \big] \\
&+ \int_{\partial\Omega} \big[e_b^1 \wedge e_2^2 - *e_1^2 \wedge f_b^1 \big] \\
&+ \int_S \big[e_d^1 \wedge f_d^2 - G_1^*(e_1^2) \wedge f_d^1 - G_2^*(e_2^2) \wedge f_d^1 \big] = 0
\end{aligned} \tag{38}$$

for all e_1^2, e_2^2, f_d^2. Now assume that e_1^2 and e_2^2 vanish on the boundary $\partial\Omega$. By (36) and Stokes' theorem, we have:

$$\begin{aligned}
&\int_\Omega \big[-e_2^2 \wedge \mathrm{d} * e_1^1 - e_1^2 \wedge *\mathrm{d}e_2^1 + e_1^2 \wedge f_1^1 + e_2^2 \wedge f_2^1 \big] \\
&\quad + \int_S \big[G_1^*(e_1^1) \wedge f_d^2 + G_2^*(e_2^1) \wedge f_d^2 + e_d^1 \wedge f_d^2 \big] \\
&\quad - \int_\Omega \big[e_1^2 \wedge G_1(f_d^1) + e_2^2 \wedge G_2(f_d^1) \big] = 0
\end{aligned} \tag{39}$$

for all e_1^2, e_2^2, f_d^2 with $e_1^2\big|_{\partial\Omega} = e_2^2|_{\partial\Omega} = 0$. Since the pairing (3) is non-degenerate, this implies

$$f_2^1 = \mathrm{d} * e_1^1 + G_2(f_d^1), \tag{40a}$$
$$f_1^1 = *\mathrm{d}e_2^1 + G_1(f_d^1), \tag{40b}$$
$$e_d^1 = -G^* \begin{bmatrix} e_1^1 \\ e_2^1 \end{bmatrix}. \tag{40c}$$

We now release the restriction $e_1^2\big|_{\partial\Omega} = e_2^2|_{\partial\Omega} = 0$ and substitute (40) into (38). Using (36) and Stokes' theorem, we obtain

$$\int_{\partial\Omega} \big[*e_1^1 \wedge e_2^2 + *e_1^2 \wedge e_2^1 + e_b^1 \wedge e_2^2 - *e_1^2 \wedge f_b^1 \big] = 0 \tag{41}$$

for all e_1^2, e_2^2. This implies $e_b^1 = - * e_1^1\big|_{\partial\Omega}$ and $f_b^1 = e_2^1\big|_{\partial\Omega}$. Thus $(f^1, e^1) \in \mathcal{D}$. ∎

REFERENCES

[1] A. van der Schaft, "L_2-Gain and Passivity Techniques in Nonlinear Control," Springer, 2000.

[2] B. Brogliato, R. Lozano, B. Maschke, and O. Egeland, "Dissipative Analysis and Control," Springer, 2nd Edition, 2007.

[3] A.J. van der Schaft and B.M. Maschke, "Hamiltonian formulation of distributed-parameter systems with boundary energy flow," *J. Geom. Phys.*, vol. 42, pp. 166–194, 2002.

[4] B. Jacob and H.J. Zwart, "Linear Port-Hamiltonian Systems on Infinite-Dimensional Spaces," Birkhuser, 2012.

[5] G. Golo, V. Talasila, A. van der Schaft, and B. Maschke, "Hamiltonian discretization of boundary control systems," *Automatica*, vol. 40, pp. 757–771, 2004.

[6] R. Lopezlena and J.M.A. Scherpen, "Lumped approximation of a transmission line with an alternative geometric discretization," Proceedings of the *2nd IFAC Symp. on Systems, Structure and Control*, Oaxaca, Mexico, pp. 418–423, 2004.

[7] M. Seslija, A.J. van der Schaft and J.M.A. Scherpen, "Discrete exterior geometry approach to structure-preserving discretization of distributed-parameter port-Hamiltonian systems," *J. Geom. Phys.*, vol. 62, pp. 1509–1531, 2012.

[8] A. Bossavit, "Discretization of electromagnetic problems: The 'generalized finite differences' approach," in: *Handbook of Numerical Analysis XIII, Special Volume: Numerical Methods in Electromagnetics*, pp. 105–197, 2005.

[9] O. Farle, D. Klis, M. Jochum, O. Floch and R. Dyczij-Edlinger, "A port-Hamiltonian finite-element formulation for the Maxwell equations," Proceedings of the *2013 International Conference on Electromagnetics in Advanced Applications* (ICEAA), pp. 324–327, 2013.

[10] D. Boffi, F. Brezzi and M. Fortin, "Mixed Finite Element Methods and Applications," Springer, 2013.

[11] D. Jeltsema and J.M.A. Scherpen, "Multidomain modeling of nonlinear networks and systems," *IEEE Control Syst. Mag.*, vol. 29, pp. 28–59, 2009.

[12] D.N. Arnold, R.S. Falk, and R. Winther, "Finite element exterior calculus: From Hodge theory to numerical stability," *Bull. Amer. Math. Soc.*, vol. 47, pp. 281–345, 2010.

[13] P.J. Olver, "Application of Lie Groups to Differential Equations," Springer, 2nd edition, 1993.

[14] R. Hiptmair, "Discrete Hodge operators," *Numer. Math.*, vol. 90, pp. 265–289, 2001.

[15] K. Atkinson and W. Han, "Theoretical Numerical Analysis," Springer, 3rd edition, 2009.

[16] I. Babuska, B. Szabo, and I. Katz, "The p-Version of the Finite Element Method," *SIAM Journal on Numerical Analysis*, vol. 18, no. 3, pp. 515-545, 1981.